

## RESEARCH ARTICLE

## MOLECULAR STRUCTURE

# Hydrogen atoms can be located accurately and precisely by x-ray crystallography

Magdalena Wońska,<sup>1</sup> Simon Grabowsky,<sup>2\*</sup> Paulina M. Dominiak,<sup>1</sup> Krzysztof Woźniak,<sup>1</sup> Dylan Jayatilaka<sup>3</sup>

2016 © The Authors, some rights reserved; exclusive licensee American Association for the Advancement of Science. Distributed under a Creative Commons Attribution NonCommercial License 4.0 (CC BY-NC). 10.1126/sciadv.1600192

Precise and accurate structural information on hydrogen atoms is crucial to the study of energies of interactions important for crystal engineering, materials science, medicine, and pharmacy, and to the estimation of physical and chemical properties in solids. However, hydrogen atoms only scatter x-radiation weakly, so x-rays have not been used routinely to locate them accurately. Textbooks and teaching classes still emphasize that hydrogen atoms cannot be located with x-rays close to heavy elements; instead, neutron diffraction is needed. We show that, contrary to widespread expectation, hydrogen atoms can be located very accurately using x-ray diffraction, yielding bond lengths involving hydrogen atoms (A–H) that are in agreement with results from neutron diffraction mostly within a single standard deviation. The precision of the determination is also comparable between x-ray and neutron diffraction results. This has been achieved at resolutions as low as 0.8 Å using Hirshfeld atom refinement (HAR). We have applied HAR to 81 crystal structures of organic molecules and compared the A–H bond lengths with those from neutron measurements for A–H bonds sorted into bonds of the same class. We further show in a selection of inorganic compounds that hydrogen atoms can be located in bridging positions and close to heavy transition metals accurately and precisely. We anticipate that, in the future, conventional x-radiation sources at in-house diffractometers can be used routinely for locating hydrogen atoms in small molecules accurately instead of large-scale facilities such as spallation sources or nuclear reactors.

## INTRODUCTION

The role of hydrogen in chemistry cannot be understated. The hydrogen atom commonly terminates the valences of other atoms and thus is a major constituent of the molecular surface. The hydrogen ion concentration (pH) is a control variable for chemical reactions, and H atoms play a key role in biology and medicine (1–3), with increased interest in determining their positions with x-radiation (4). In materials science, some argue that, to mitigate the consequences of human-induced climate change, hydrogen storage materials must play a key role (5).

Unfortunately, the very reason that makes H atoms so central in chemistry—the fact that they have only one electron—makes them very hard to detect with x-rays accurately because x-rays scatter from the electron density (6, 7). On the other hand, thermal neutrons diffract strongly from the nuclei of H atoms, which makes them detectable by using nuclear reactors or spallation facilities as radiation sources. However, the cost of a neutron diffraction facility is immense, the perceived risk of operating a nuclear reactor is not negligible, and the accessibility for researchers is limited. In contrast, operating an x-ray diffractometer is routine, and far more than a million structures solved by x-ray diffraction have been published.

It has been known for some time that H atoms in small molecules can, in principle, be located by x-rays (that is, refined freely without constraints or restraints), provided that high-quality and high-resolution low-temperature data are available (8, 9). This requires a change in the standard molecular and atomic model away from the 100-year-old independent atom model (IAM) (10)—a superposition of spherical

atomic electron densities—that has implemented the Stewart-Davidson-Simpson (SDS) scattering factor for the hydrogen atom (11). Instead, fixed bonded-atom polarized scattering factors for the hydrogen atom were introduced by Stewart *et al.* (12, 13) but only seldomly applied (14, 15). An extension of this idea is based on aspherical atomic electron densities in the Hansen-Coppens pseudoatom formalism [multipole modeling (16)] using databases (17–19). However, these database methods are regarded as specialist techniques. A new technique called Hirshfeld atom refinement (HAR) (20, 21) is available and can be applied as easily as the IAM. It provides improved tailor-made aspherical atomic electron densities, which are extracted from a crystal-field-embedded quantum-chemical electron density using Hirshfeld's scheme (22) (see Fig. 1). In preliminary work, it was indeed possible for two organic molecules to freely refine H atom positions and the corresponding anisotropic displacement parameters (ADPs) using x-ray diffraction and the HAR technique (21, 23), but neither accuracy and precision nor general applicability had been investigated.

The recent work and a strong interest in H atoms alluded to the question: Is it possible to obtain H atom positions and associated bond lengths accurately and precisely from routine x-ray diffraction data?

To answer this question, we refined a total of 81 crystal structures of small organic molecules from the literature using HAR and compared the obtained A–H bond lengths with averaged results obtained with neutron diffraction (24). According to Allen and Bruno (24), the A–H bonds occurring in the 81 selected crystal structures can be categorized into 24 different classes, comprising various types of C–H, O–H, and N–H bonds, plus O–H in crystal water that we considered additionally. The main selection criteria used to source the x-ray data were that they could, in principle, be obtained in a normally equipped x-ray diffraction laboratory, that the temperature was below 140 K, and that the resolution was at least 0.6 Å. Full details can be found in Materials and Methods as well as in the Supplementary Materials.

<sup>1</sup>Biological and Chemical Research Centre, Chemistry Department, University of Warsaw, Zwirki i Wigury 101, 02-089 Warszawa, Poland. <sup>2</sup>Institut für Anorganische Chemie und Kristallographie, Fachbereich 2–Biologie/Chemie, Universität Bremen, Leobener Str. NW2, 28359 Bremen, Germany. <sup>3</sup>School of Chemistry and Biochemistry, University of Western Australia, 35 Stirling Highway, Perth, Western Australia 6009, Australia.

\*Corresponding author. Email: [simon.grabowsky@uni-bremen.de](mailto:simon.grabowsky@uni-bremen.de)

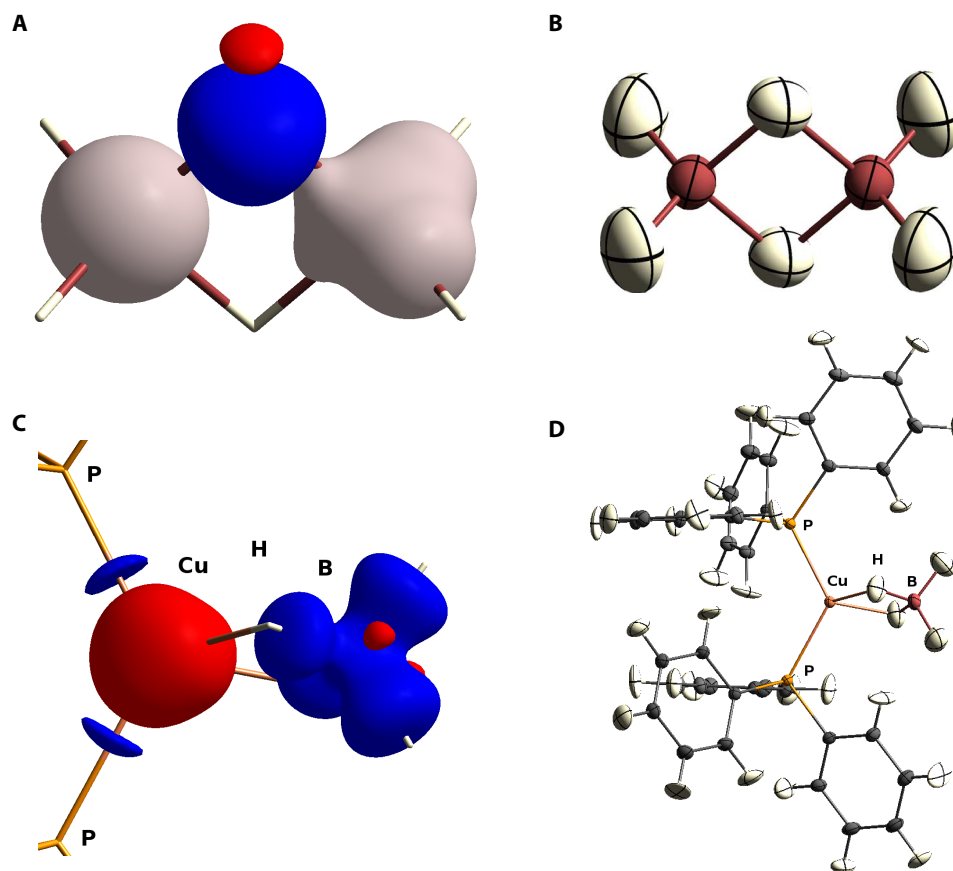


**Fig. 1. Visualization of Hirshfeld atoms and deformation Hirshfeld densities.** (A) For diborane  $B_2H_6$  (25), isosurfaces ( $\rho = 0.08 \text{ e}/\text{\AA}^3$ ) of the boron electron density used to calculate the atomic scattering factors in the IAM (left, spherical, gray) and in HAR (right, aspherical, gray) are shown. The latter is a representation of the Hirshfeld atom. Bonding effects are neglected in the IAM by using a sphere but are accounted for in HAR by using Hirshfeld's stockholder partitioning (22). The deformation Hirshfeld density (difference between the Hirshfeld density and the spherical density) is depicted for one of the bridging H atoms ( $\rho = 0.006 \text{ e}/\text{\AA}^3$ ). Blue represents positive deformation Hirshfeld density (that is, regions that gain electron density upon the transition from a spherical to an aspherical atom representation); red represents negative deformation Hirshfeld density (that is, regions that lose electron density upon the transition). (B) The resulting HAR-based molecular structure of diborane with ADPs for all atoms, including hydrogen atoms, is shown at a 50% probability level. (C) In (tetrahydroborato)bis(triphenylphosphine)copper(I) (26), deformation Hirshfeld densities ( $\rho = 0.006 \text{ e}/\text{\AA}^3$ ) are shown for copper and boron atoms. For color code, see (A). Both atoms gain electron density in the bonding regions. The extent of this effect is an indicator for the degree of covalent bonding, and it is the reason for the improved A–H bond description. (D) The resulting HAR-based molecular structure of the compound in (C) with ADPs for all atoms, including hydrogen atoms, is shown at a 50% probability level.

## RESULTS

In Fig. 2, we present statistical analyses of the comparisons of A–H bond lengths between x-ray diffraction (HAR and IAM) and neutron diffraction derived values. All HAR results come from a fully anisotropic model for all atomic displacements, including hydrogen atom ADPs, which is impossible in the IAM. Details of the statistics applied are described in Materials and Methods. There is remarkably good agreement between the averaged bond lengths from HAR and neutron refinements in Fig. 2. The differences between the means are always less than two HAR sample SDs, and smaller than one HAR sample SD for all bond types with at least 30 representatives in the x-ray sample (see the right-hand column in Fig. 2 for the sample number). This agreement represents a fundamental improvement in the results obtained from the routinely used IAM (also shown in Fig. 2). Mean bond lengths from IAM deviate significantly from the accurate HAR and neutron results.

Despite these encouraging results, the two-sided Welch test (27) shows that, for most bond types, the mean bond lengths from HAR and neutron diffraction are not equal within a 95% confidence interval. In almost all cases, the HAR values are systematically smaller, and the difference between the individual means is, on average, between 0.01 and 0.02 Å. Therefore, the one-sided Welch test (27) was applied to further investigate the cases in which the hypothesis of equality of neutron and HAR means was rejected. At a 5% significance level, the differences between neutron and HAR means exceed the confidence interval by 0.001 to 0.020 Å; however, this deviation is within a single SD for each bond type and refinement strategy. This means that, if the averaged bond lengths agree within 0.020 Å, then statistical equivalence would be achieved. Hence, the actual achieved agreement of 0.01 to 0.02 Å is within the value for strict statistical agreement. This level of agreement can be understood as a measure of the accuracy of the HAR procedure if the results from neutron diffraction are considered as the

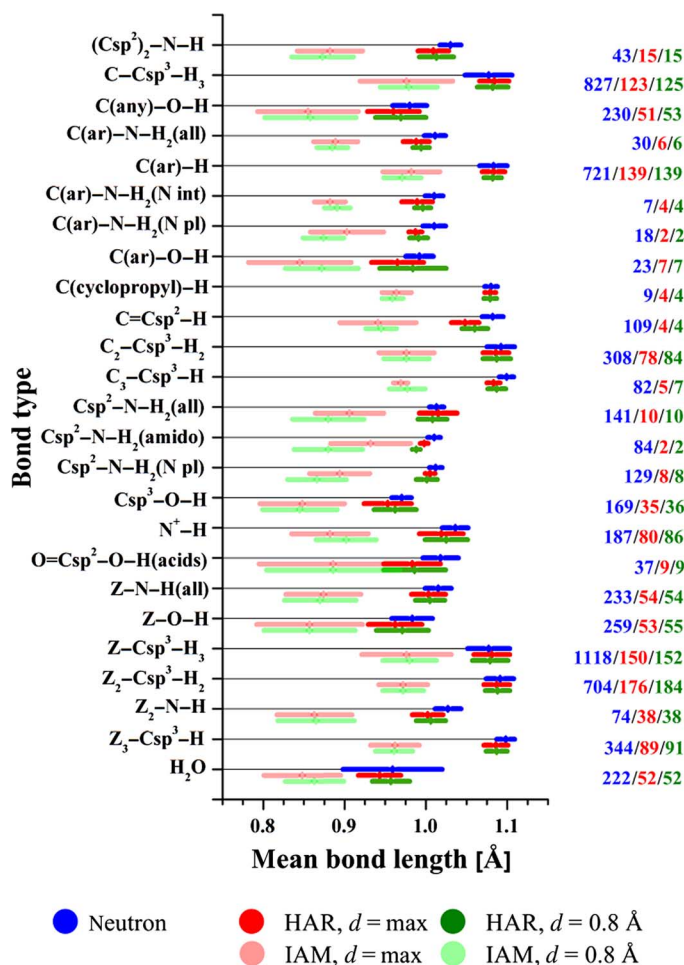


**Fig. 2. Analysis of A-H bond lengths.** Averaged A-H bond lengths with sample standard deviations (SDs) obtained from neutron diffraction versus those obtained from x-ray diffraction (HAR and IAM models) at restricted resolution ( $d = 0.8 \text{ \AA}$ ) and with no restriction ( $d = \max$ ). Twenty-four bond classes  $Z_n$ -A-H are taken from Allen and Bruno (24) and indicate the atom A bonded to the H atom, and in the case of  $A=C$ , the hybridization and the number of atoms Z of any kind with  $n = 1, 2, 3$  bonded to the C atom. For cocrystallized water, we averaged O-H bond lengths obtained from neutron diffraction using entries in the Cambridge Structural Database (CSD). The numbers of observations for all bond types for each refinement method are given in the same color code in the right-hand column. For more details on the statistical analyses, see Materials and Methods. For more analyses and representations, see the Supplementary Materials.

reference values. However, this is only an approximation of accuracy because we do not compare individual refined H atom positions but H atoms in a class. Nevertheless, the IAM x-ray results are shorter by about  $0.12 \text{ \AA}$  on average, referenced to the neutron results, which is an order of magnitude more inaccurate than the HAR results. Multipole modeling of all 81 data sets included in this study was out of scope because significantly more user interaction is required here than in HAR, even if multipole databases are applied. However, multipole-model-derived bond lengths on some selected examples agree more closely with the neutron results than IAM-derived bond lengths, but an agreement of  $0.01$  to  $0.02 \text{ \AA}$  was not reached. We will present more detailed comparisons between HAR and multipole modeling in a forthcoming study.

Sample standard deviations (SDs) (error bars in Fig. 2) can be used as a measure of the precision of determining the A-H bond lengths within each bond class. Again, this is an approximation to precision because the spread of the values can be influenced by actual chemical effects, such as intermolecular interactions, or physical effects caused by, for example, difference in the temperature of measurements. Nevertheless, Fig. 2 shows in this context that the results from neutron diffraction are only slightly more precise than the HAR results, with the SDs always being in the same order of magnitude. This finding is contrary to the intuition that neutron diffraction experiments provide significantly more precise H atom parameters. The results from IAM treatment are clearly less precise as well as less accurate. The case of the O-H bonds in cocrystallized water is exceptional (last row in Fig. 2): The spread of values can be reduced drastically for water, which is prone to be involved in hydrogen bonds, by using a different refinement method, namely, HAR applied to x-ray data and not neutron diffraction. Therefore, only part of the spread can be caused by chemical features, and the difference in the SD shows that HAR is notably more precise than neutron diffraction for water.

To test the effect of resolution on the A-H bond lengths, we performed refinements at the respective maximum resolution of each data set and at resolutions of  $0.6, 0.7,$  and  $0.8 \text{ \AA}$ . Figure 2 summarizes the results for the highest (max) and lowest ( $0.8 \text{ \AA}$ ) resolutions. The accuracy and precision of hydrogen atom positions obtained for the lowest resolution are as good as those obtained for the maximum resolution. Although the fact that all evaluated compounds scattered to at least  $0.6 \text{ \AA}$  in the measurement means that our selection does not represent the average routine data set for structure determination that might only be resolved to a maximum of  $0.8 \text{ \AA}$ , successful refinement of every data set pruned to  $0.8 \text{ \AA}$  is a significant result. It renders it possible, in the future, to routinely apply HAR to data sets for standard small-molecule structure elucidation.

Only for organic compounds are there enough available equivalent neutron and x-ray data sets to perform meaningful statistical analyses. For A-H bonds in inorganic compounds, only a proof of principle for selected compounds of interest can be presented herein, including bridging H atoms and H atoms bonded to heavy transition metals (Table 1). A significant elongation of all A-H bonds between HAR and IAM treatments is observed, which means improved accuracy relative to the reference values accompanied by significant improvement in precision. For elements up to argon, HAR is as easy as for organic compounds, whereas HAR treatments with heavier elements can fail because they are technically not simple and beyond routine applicability at present. This includes problems with the availability of suitable all-electron basis sets for atoms beyond period 4 and related issues with obtaining a robust electron density for these systems, as well as problems with the availability of good-quality x-ray data sets that provide starting positions for hydrogen atoms bonded to heavy elements. However, Table 1 and Fig. 1D show that the method is, in principle, able to locate H atoms accurately and precisely next to transition metals as heavy as ruthenium and platinum, which are both known to be potent catalysts for hydrogen activation (28).

The total number of individual hydrogen ADPs in all the structures subjected to HAR amounted to 1001, and 94 to 99% of them (depending on the applied resolution cutoff) belonged to successfully refined data sets. Therefore, hydrogen ADPs can generally be refined to convergence. The A-H bond lengths determined from anisotropic refinements are in slightly better agreement with the neutron-derived A-H results than those from isotropic refinements for the resolution  $0.8 \text{ \AA}$  (by  $0.003 \text{ \AA}$ ), whereas for all the other resolution ranges, there is no difference (see tables S1 to S66 in the extended supplementary document "Raw refinement and

**Table 1. A–H bond lengths in inorganic compounds (terminal and bridging).** Bond lengths in (Å) stem from both IAM and HAR treatments. Reference values given in brackets are not from neutron diffraction experiments on the same compound. \*All IAM values are based on our own refinements using the published structure factors and isotropic hydrogen displacements, whereas the HAR results are based on fully anisotropic refinements, including the H atoms (except for METRAF and AGOZEC, for which isotropic hydrogen displacements were used). †In the literature, there is a surprising lack of neutron diffraction studies for inorganic molecular compounds. Theoretical calculations cannot serve as references because even MP4 or CCSD(T) are never more precise than 0.01 Å in terms of bond length determination (29). ‡From electron diffraction in the gas phase, compare Hübschle *et al.* (25). §New crystal structure determination for this study; see Materials and Methods for more details. ¶Neutron diffraction of different compounds with terminal Si–H bonds (REFCODES: UJABOX01 and COQYUC01). ¶¶Here, only the Cambridge Crystallographic Data Centre (CCDC) REFCODE of the original crystal structure is given; see Materials and Methods for more details on the compound and the original publication. #Averaged over seven structures from neutron diffraction (REFCODES: HINBOV01, HIPBAL01, MIGKIY01, NEBNEO, OGEFIR01, UJABOX01, and ZEGYUF01) with a total of 12 terminal Ru–H bonds; the value in brackets is the sample SD—in all other cases, it is the least-squares estimated standard uncertainty. \*\*Neutron diffraction of a different compound with a terminal Pt–H bond (REFCODE: CAKNEH01). No standard uncertainties on the coordinates were given. N/A, not available.

		IAM*	HAR*	Reference <sup>†</sup>
Diborane (25) (see Fig. 1)	<b>B–H bridging</b>	1.229(5) and 1.248(5)	1.296(6) and 1.296(6)	[1.339(6) and 1.339(6)] <sup>‡</sup>
	<b>B–H terminal</b>	1.052(6) and 1.053(6)	1.170(7) and 1.168(6)	[1.196(8) and 1.196(8)] <sup>‡</sup>
BHTPCU12 (26) (see Fig. 1)	<b>B–H bridging</b>	1.186(18)	1.264(7)	N/A
	<b>B–H terminal</b>	1.093(17)	1.209(7)	N/A
	<b>Cu–H bridging</b>	1.802(18)	1.809(7)	N/A
Pentaphenyldisiloxane <sup>§</sup>	<b>Si–H</b>	1.391(12)	1.482(9)	[1.481(5), 1.506(2)] <sup>¶</sup>
QOSZON <sup>¶</sup>	<b>Fe–H</b>	1.421(21)	1.414(8)	1.521(2)
	<b>Fe–H</b>	1.442(22)	1.531(9)	1.529(2)
AGOZEC <sup>¶</sup>	<b>Ru–H</b>	1.589(15)	1.707(18)	[1.694(71)] <sup>#</sup>
METRAF <sup>¶</sup>	<b>Pt–H</b>	1.601(43)	1.686(4)	[1.610]**

statistical data”). This is true even if the quality of the hydrogen ADPs (judged by visual inspection) is poor in some cases. Obliqueness and oblateness of hydrogen ADPs occur much more frequently after anisotropic HAR than, for example, after modeling via transfer from neutron-based data as implemented in the SHADE method (30). However, contrary to all other methods (31, 32), in HAR the ADPs are obtained only from information derived from the x-ray data for the particular compound.

For an independent check and a quantification of the quality of the hydrogen ADPs, we used the checkCIF service normally used for quality control when submitting crystal structures for publication (<http://checkcif.iucr.org>), which emits “alerts” (labeled A, B, and C) of successively decreasing severity. The specific meaning of the alerts in terms of ellipsoid dimensions and the detailed analysis of the hydrogen ADPs for each structure can be found in the extended supplementary document “Raw refinement and statistical data” (tables S67 to S70). For example, nonpositive definite ADPs are reported as alert A if found in the main molecule. The percentage of hydrogen ADPs causing the most serious alert A is at 4% for the maximum and 0.6-Å resolutions and grows with further decreasing resolution, attaining 5% at 0.7 Å and 9% at 0.8 Å. The fraction of alert B and alert C ADPs, which are unlikely to signify major refinement problems, remains constant for different resolutions and amounts to approximately 1 to 2% and 5 to 6%, respectively.

## DISCUSSION

HAR is carried out with the free software Tonto (33) [HARt (HAR terminal) subprogram, <http://github.com/dylan-jayatilaka/tonto>],

which has recently been incorporated into the free crystallographic program Olex2 (34) ([www.olexsys.org](http://www.olexsys.org)). HAR treatments amount to several hours for small organic compounds to several days for bigger molecules on current single-processor desktop workstations. We do not expect this to be a serious problem in the near future because the availability of many-processor computing is becoming ubiquitous. Here, a refinement was considered successful if the least-squares procedure was convergent and the molecular structure was conserved. Among all performed refinements (different resolution, different hydrogen atom treatment), 97% of the refinements were successful. Ultimately, 75 of 81 data sets (93%) could be refined successfully, regardless of resolution or atomic anisotropy treatment. For some of the data sets with failures, HAR helped to unravel experimental problems. Hence, in total, three individual refinements are regarded as true failures of the HAR procedure.

Application of HAR to network structures, disordered compounds, or molecular biology is not yet possible. Moreover, apart from code optimizations within HAR, improvements in measurement techniques and better accuracy of data collection and reduction are necessary. However, this study shows that HAR is easily accessible and successful. It can be performed from now on as the last step of most small-molecule crystal structure determinations, which is of huge interest for every scientist using x-ray crystallography as an analytical tool because it will yield H atom positions that are as accurate and precise as those derived from neutron diffraction experiments. Accurately and precisely locating all the atomic positions, but especially those of hydrogen atoms, is moreover crucial as a starting point for electron density or x-ray wave-

function refinements that give access to properties that cannot be generally obtained from traditional crystallographic refinements, such as energies of interactions. We therefore believe that HAR is one of the central milestones in the evolving field of quantum crystallography.

## MATERIALS AND METHODS

### Experimental design

Eighty-one data sets of organic compounds were selected from various sources and subjected to HAR. The selection was restricted by the following conditions:

- 1 Only published data sets. Details, CCDC REFCODES, and assignment to references [(14, 21, 23, 32, 46–92)] are given in table S1.
- 2 Only x-ray data sets of at least  $d = 0.6 \text{ \AA}$ , to test the effect of resolution.
- 3 Temperature of experiment not higher than 140 K.
- 4 Purely organic compounds with no metal ions.
- 5 Absence of disorder (except water molecules with fractional occupancy in the structures).
- 6 No anharmonic motion reported.
- 7 Only data available in *Acta Crystallographica* journals.

With the above restrictions 1–7, we found 60 data sets. The earliest data were from 1988. Because the location of H atoms is particularly important for biology, we selected some additional data (not always in *Acta Crystallographica*): four amino acids, one dipeptide, six tripeptides, benzene, sucrose, and urea. Because they were used in a recent detailed study of HAR, we also included data for the dipeptide Gly-L-Ala with a slightly lower resolution of  $0.657 \text{ \AA}$ .

Some crystal structures appeared multiple times. For those, the bond lengths used in the analysis were the weighted averages with corresponding weighted SDs. Three of them contained two molecules of the main compound per asymmetric unit (so-called  $Z' = 2$  structures). In further 23 structures, a solvent molecule (mostly water) was also present. The only atoms appearing other than C, N, O, and H were S (six compounds), P (two compounds), F (one compound), and Cl (four compounds). No H atoms bonded to S or P were present.

Full details of the compounds with relevant information (source for the list of measured reflection data, structure, literature references, HAR details, and previous high-resolution refinement details) are presented in table S1 and in the extended supplementary document “Raw refinement and statistical data” (including representations of the HAR-refined geometries with anisotropic atomic displacement ellipsoids), which has been deposited at [www.figshare.com](http://www.figshare.com) and can be obtained under <https://dx.doi.org/10.6084/m9.figshare.3205588.v1>.

The inorganic compounds were selected to include hydrogen atoms in quite different environments: bonded to second- to sixth-row elements, in bridging and terminal positions. The data for diborane stemming from a charge-density study (25) were made available by C. B. Hübschle (University of Bayreuth). We measured data for pentaphenyldisiloxane at beamline D3 of storage ring DORIS III at the HASYLAB (Hamburger Synchrotronstrahlungslabor) of DESY (Deutsches Elektronen-Synchrotron) in Hamburg [triclinic  $P\bar{1}$ ,  $Z = 2$ ,  $a = 9.110(2) \text{ \AA}$ ,  $b = 10.543(2) \text{ \AA}$ ,  $c =$

$13.597(3) \text{ \AA}$ ,  $\alpha = 94.30(3)^\circ$ ,  $\beta = 106.90(3)^\circ$ ,  $\gamma = 92.96(3)^\circ$ ,  $V = 1242.3(5) \text{ \AA}^3$ ;  $T = 8(1) \text{ K}$ ,  $\lambda = 0.5166(2) \text{ \AA}$ ,  $d_{\text{max}} = 0.45 \text{ \AA}$ ; number of collected reflections = 273,011; number of unique reflections = 25,392; completeness of data = 89.2%;  $R_{\text{int}} = 0.063$ ]. More details will be reported in a forthcoming study. Data for further inorganic compounds were retrieved from *Acta Crystallographica* publications (unless otherwise stated) and subjected to HAR: (tetrahydroborato)bis(triphenylphosphine) copper(I) (REFCODE: BHPTCU12) (26), [1,1-bis(diphenylphosphino)ferrocene]-carbonyl[dihydrobis(pyrazol-1-yl)-borato]hydridoruthenium(II) acetone solvate (REFCODE: AGOZEC) (35), dicarbonyl-*cis*-dihydro-*trans*-bis(triphenylphosphite-O)-iron(II) (REFCODE: QOSZON; data made available by V. Arion, University of Vienna) (36), and *trans*-bromohydridobis(triphenylphosphine)-platinum(II) (REFCODE: METRAF) (37).

### Hirshfeld atom refinement

The HAR method of crystallographic structural refinement uses aspherical atomic scattering factors obtained from the quantum-mechanical electron density of a molecule in a simulated crystal environment. This requires only single-molecule calculations. Full details have been published elsewhere (20, 21). For most of the structures, refinement was performed starting from the initial geometry obtained from the literature. For calculations of molecular wave functions in HAR, the central moiety was embedded in a cluster of charges and dipoles on all atoms on all surrounding molecules with at least one atom within the radius of  $8 \text{ \AA}$ . The wave function was calculated using density functional theory (38) with the Becke-Lee-Yang-Parr functional (39, 40). The correlation-consistent polarized valence double- $\zeta$  (cc-pVDZ) basis set (41) was chosen for the unconstrained refinement of hydrogen positions in crystals because it was previously shown to be sufficient (21). The refinement was performed on structure factor magnitudes ( $F$ ) using only the reflections with  $F > 4\sigma(F)$ . Coordinates of all the atoms, including hydrogen atoms, were freely refined. ADPs of all nonhydrogen atoms were always refined, whereas, as far as hydrogen atoms are concerned, two versions of each refinement were carried out—with anisotropic and isotropic treatment of hydrogen displacement parameters. In contrast to other programs for structure refinement, in the program HART, the unique  $U_{\text{iso}}$  value is not explicitly refined as a separate parameter but obtained by removing linear combinations of redundant parameters in the least-squares matrix. Therefore, in nonorthogonal crystal systems, the isotropic displacement parameter is not diagonal; compare Eq. 44 in Trueblood *et al.* (42). Furthermore, for each organic compound, the refinement was performed on four sets of reflections: for the maximum resolution (different for various structures) and for three resolution cutoffs: 0.6, 0.7, and  $0.8 \text{ \AA}$ . For the inorganic compounds, only the maximum resolution was used. Instead of the cc-pVDZ basis set, DZP according to Barros *et al.* (43) was used for Ru and DZP according to de Berrêdo and Jorge (44) was used for Pt. Crystallographic information files (CIFs) for all refinements are deposited with this article as supplementary information. The isotropic refinement at maximum resolution for each compound has been submitted as CIF to the CSD (see table S1 for the deposition numbers) and can be obtained free of charge at [www.ccdc.cam.ac.uk](http://www.ccdc.cam.ac.uk). A CIF including the anisotropic refinement of diborane was deposited with the Inorganic Crystal Structure Database (deposition no. CSD-430202) and can be obtained at <http://icsd.fiz-karlsruhe.de>.

### Statistical analysis

A–H bonds (C–H, O–H, and N–H bonds) present in the refined crystal structures of the organic compounds were grouped into bond types

identified in the course of a similar analysis performed for neutron A–H bonds by Allen and Bruno (24). Their work gives access only to the values of the averaged neutron bond lengths, their sample SDs, and the numbers of observations in the sample, without revealing the values of individual observations. For this reason and also because of the very limited number of crystalline structures for which both neutron and x-ray experimental data are available, only a comparison between averaged neutron and averaged x-ray A–H bond lengths can be done, if the condition of a statistically meaningful number of bonds representing each bond type is to be fulfilled. In the article by Allen and Bruno (24), two different classes of bond types were defined—a class containing only eight general bond types detailed in table 4 of the cited article [ $Z^3\text{-Csp}^3\text{-H}$ ,  $Z^2\text{-Csp}^3\text{-H}^2$ ,  $Z\text{-Csp}^3\text{-H}^3$ ,  $\text{Csp}^2$  or  $\text{C(ar)-H}$ ,  $\text{C(ar)-H}$ ,  $Z\text{-O-H}$ ,  $Z\text{-N-H}$ , and  $\text{N}^+\text{-H}$ , where Z stands for any element except H and C(ar) denotes aromatic carbon; otherwise, hybridization of carbon is given in italics] and a class containing more specific bond types collected in their table 2, 24 of which were identified in the analyzed data sets. In the case of table 4, the values from columns containing averages based on experimental results from the temperature ranges  $T \leq 60$  K and  $60 \leq T \leq 140$  K were merged for comparison with the corresponding x-ray HAR averages. For each bond type, a statistically significant number of observations higher than 50 was achieved for the x-ray data, enabling a reliable comparison between x-ray and neutron bond lengths. This was not the case for the 24 bond types identified according to table 2, for half of which the number of representatives in the x-ray HAR statistic was smaller than 30 and for which four types were substantially underrepresented in the neutron results. For those bond types, only a rough comparison can be made, allowing, however, to gain certain insight into the performance of HAR for H atoms in more specific chemical groups. Additionally, the O–H bond in cocrystallized water molecules is included in the study. In this case, a suitable statistic was performed on the basis of water-containing molecular neutron structures deposited with the CSD, according to the guidelines described in the work of Allen and Bruno (24).

The comparison of the neutron and x-ray HAR A–H bond lengths was based on the averaged values obtained for the defined bond types and their sample SDs. For the HAR bond lengths, the performed Shapiro-Wilk test (45) proved that, in many cases, the assumption of normality is not fulfilled. For the neutron bond lengths, only averaged values and SDs were available; thus, neither testing of the data for normality nor performance of nonparametric statistical tests was possible. Therefore, the final choice for testing the equality of neutron and x-ray HAR mean bond lengths was Welch's  $t$  test (27); it is used to compare two samples with unequal variances and is suitable if the means of the samples are approximately normally distributed. According to the central limit theorem, the means of a sample with finite variance converge to the normal distribution, with the sample size approaching infinity, irrespective of the actual distribution of the population. It is customary to assume that, for sufficiently large samples (that is, at least 30 observations), the distribution of their means is approximately normal. This assumption is valid for all the bond types in fig. S1 (C and D) and for half of the bond types in Fig. 1 as well as fig. S1 (A and B). For the remaining bond types, the results of the Welch test are only approximations and are presented here to give a general view of the performance of the method in more scarcely encountered bond types. The two-sided Welch test (assumed significance level of 5%) was used to decide on the equality of the neutron and x-ray HAR means. In those cases in which the hypothesis on equality was rejected, the biggest possible difference

between x-ray and neutron means was calculated (from the one-sided Welch test) so that the two means would agree (at the same significance level). The results can be found in the extended supplementary document “Raw refinement and statistical data” (tables S1 to S66).

## SUPPLEMENTARY MATERIALS

Supplementary material for this article is available at <http://advances.sciencemag.org/cgi/content/full/2/5/e1600192/DC1>

fig. S1. Averaged A–H bond lengths and mean x-ray–neutron bond length differences.

table S1. Information on the compounds used for HAR.

Further raw data are deposited as additional supplementary materials with *Science Advances* or with the service [www.figshare.com](http://www.figshare.com):

1) Raw refinement and statistical data as a separate PDF document, deposited at [www.figshare.com](http://www.figshare.com) under <https://dx.doi.org/10.6084/m9.figshare.3205588.v1>.

2) Crystallographic information files (CIFs) of all refinements in native text format

## REFERENCES AND NOTES

1. R. E. Hubbard, M. Kamran Haider, *Hydrogen Bonds in Proteins: Role and Strength* (eLS Wiley, Chichester, UK, 2010).
2. J. U. Bowie, Membrane protein folding: How important are hydrogen bonds? *Curr. Opin. Struct. Biol.* **21**, 42–49 (2011).
3. E. T. Kool, Hydrogen bonding, base stacking, and steric effects in DNA replication. *Annu. Rev. Biophys. Biomol. Struct.* **30**, 1–22 (2001).
4. H. Ogata, K. Nishikawa, W. Lubitz, Hydrogens detected by subatomic resolution protein crystallography in a [NiFe] hydrogenase. *Nature* **520**, 571–574 (2015).
5. P. Jena, Materials for hydrogen storage: Past, present, and future. *J. Phys. Chem. Lett.* **2**, 206–211 (2011).
6. M. Schmidtman, P. Coster, P. F. Henry, V. P. Ting, M. T. Weller, C. C. Wilson, Determining hydrogen positions in crystal engineered organic molecular complexes by joint neutron powder and single crystal X-ray diffraction. *CrystEngComm* **16**, 1232–1236 (2014).
7. P. Müller, R. Herbst-Irmer, A. L. Spek, T. R. Schneider, M. R. Sawaya, Hydrogen atoms, in *Crystal Structure Refinement: A Crystallographer's Guide to SHELXL*, P. Müller, Ed. (International Union of Crystallography Texts on Crystallography, Oxford University Press, New York, no. 8, 2006), chap. 3.
8. A. A. Hoser, P. M. Dominiak, K. Woźniak, Towards the best model for H atoms in experimental charge-density refinement. *Acta Crystallogr.* **A65**, 300–311 (2009).
9. A. Ø. Madsen, Modeling and analysis of hydrogen atoms. *Struct. Bond.* **146**, 21–52 (2012).
10. A. H. Compton, The distribution of electrons in atoms. *Nature* **95**, 343–344 (1915).
11. R. F. Stewart, E. R. Davidson, W. T. Simpson, Coherent X-ray scattering for the hydrogen atom in the hydrogen molecule. *J. Chem. Phys.* **42**, 3175–3187 (1965).
12. J. Bentley, R. F. Stewart, Two-center calculations for X-ray scattering. *J. Comput. Phys.* **11**, 127–145 (1973).
13. R. F. Stewart, J. Bentley, B. Goodman, Generalized X-ray scattering factors in diatomic molecules. *J. Chem. Phys.* **63**, 3786–3793 (1975).
14. R. Destro, R. E. Marsh, R. Bianchi, A low-temperature (23 K) study of L-alanine. *J. Phys. Chem.* **92**, 966–973 (1988).
15. C. Gatti, E. May, R. Destro, F. Cargnoni, Fundamental properties and nature of CH–O interactions in crystals on the basis of experimental and theoretical charge densities. The case of 3,4-bis(dimethylamino)-3-cyclobutene-1,2-dione (DMACB) crystal. *J. Phys. Chem. A* **106**, 2707–2720 (2002).
16. N. K. Hansen, P. Coppens, Testing aspherical atom refinements on small-molecule data sets. *Acta Crystallogr.* **A34**, 909–921 (1978).
17. B. Zarychta, V. Pichon-Pesme, B. Guillot, C. Lecomte, C. Jelsch, On the application of an experimental multipolar pseudo-atom library for accurate refinement of small-molecule and protein crystal structures. *Acta Crystallogr.* **A63**, 108–125 (2007).
18. A. Volkov, M. Messerschmidt, P. Coppens, Improving the scattering-factor formalism in protein refinement: Application of the University at Buffalo Aspherical-Atom Databank to polypeptide structures. *Acta Crystallogr.* **D63**, 160–170 (2007).
19. B. Dittrich, C. B. Hübschle, K. Pröpper, F. Dietrich, T. Stolper, J. J. Holstein, The generalized invariom database (GID). *Acta Crystallogr.* **B69**, 91–104 (2013).
20. D. Jayatilaka, B. Dittrich, X-ray structure refinement using aspherical atomic density functions obtained from quantum-mechanical calculations. *Acta Crystallogr.* **A64**, 383–393 (2008).
21. S. C. Capelli, H.-B. Bürgi, B. Dittrich, S. Grabowsky, D. Jayatilaka, Hirshfeld atom refinement. *IUCrJ* **1**, 361–379 (2014).
22. F. L. Hirshfeld, Bonded-atom fragments for describing molecular charge densities. *Theor. Chim. Acta* **44**, 129–138 (1977).

23. M. Woińska, D. Jayatilaka, M. A. Spackman, A. J. Edwards, P. M. Dominiak, K. Woźniak, E. Nishibori, K. Sugimoto, S. Grabowsky, Hirshfeld atom refinement for modeling strong hydrogen bonds. *Acta Crystallogr.* **A70**, 483–498 (2014).
24. F. H. Allen, I. J. Bruno, Bond lengths in organic and metal-organic compounds revisited: X-H bond lengths from neutron diffraction data. *Acta Crystallogr.* **B66**, 380–386 (2010).
25. C. B. Hübschle, M. Messerschmidt, D. Lentz, P. Luger, Neubestimmung der Ladungsdichte und topologische Analyse von  $\beta$ -Diboran bei 94K. *Z. Anorg. Allg. Chem.* **630**, 1313–1316 (2004).
26. J. Moncol, M. Gembicky, P. Coppens, (Tetrahydroborato)bis(triphenylphosphine)copper(I): A redetermination at 90 K. *Acta Crystallogr.* **E61**, m242–m243 (2005).
27. B. L. Welch, The generalization of "Student's" problem when several different population variances are involved. *Biometrika* **34**, 28–35 (1947).
28. G. J. Kubas, *Metal Dihydrogen and  $\sigma$ -Bond Complexes* (Modern Inorganic Chemistry, Kluwer Academic/Plenum Publishers, New York, 2001).
29. T. Helgaker, P. Jørgensen, J. Olsen, *Molecular Electronic Structure Theory* (Wiley, New York, 2000).
30. A. Ø. Madsen, SHADE web server for estimation of hydrogen anisotropic displacement parameters. *J. Appl. Crystallogr.* **39**, 757–758 (2006).
31. P. Munshi, A. Ø. Madsen, M. A. Spackman, S. Larsen, R. Destro, Estimated H-atom anisotropic displacement parameters: A comparison between different methods and with neutron diffraction results. *Acta Crystallogr.* **A64**, 465–475 (2008).
32. A. Ø. Madsen, H. O. Sørensen, C. Flensburg, R. F. Stewart, S. Larsen, Modeling of the nuclear parameters for H atoms in X-ray charge-density studies. *Acta Crystallogr.* **A60**, 550–561 (2004).
33. D. Jayatilaka, D. J. Grimwood, *Tonto: A Fortran-Based Object-Oriented System for Quantum Chemistry and Crystallography* (Springer, New York, 2003).
34. O. V. Dolomanov, L. J. Bourhis, R. J. Gildea, J. A. K. Howard, H. Puschmann, OLEX2: A complete structure solution, refinement and analysis program. *J. Appl. Crystallogr.* **42**, 339–341 (2009).
35. S. Huh, A. J. Lough, [1,1'-Bis(diphenylphosphino)ferrocene]-carbonyl[dihydrobis(pyrazol-1-yl)-borato]hydridoruthenium(II) acetone solvate. *Acta Crystallogr.* **E64**, m1544–m1545 (2008).
36. V. Arion, J.-J. Brunet, D. Nelbecker, Crystal structure, Mössbauer spectra, and thermal behavior of  $\text{H}_2\text{Fe}(\text{CO})_2[\text{P}(\text{O}(\text{Ph})_3)_2]$ . *Inorg. Chem.* **40**, 2628–2630 (2001).
37. A. Sivaramakrishna, H. Su, J. R. Moss, *trans*-Bromohydriddibis(triphenylphosphine)platinum(II). *Acta Crystallogr.* **E63**, m244–m245 (2007).
38. P. Hohenberg, W. Kohn, Inhomogeneous electron gas. *Phys. Rev.* **136**, B864–B871 (1964).
39. A. D. Becke, Density-functional thermochemistry. III. The role of exact exchange. *J. Chem. Phys.* **98**, 5648–5652 (1993).
40. C. Lee, W. Yang, R. G. Parr, Development of the Colle-Salvetti correlation-energy formula into a functional of the electron density. *Phys. Rev. B* **37**, 785–789 (1988).
41. T. H. Dunning Jr., Gaussian basis sets for use in correlated molecular calculations. I. The atoms boron through neon and hydrogen. *J. Chem. Phys.* **90**, 1007–1023 (1989).
42. K. N. Trueblood, H.-B. Bürgi, H. Burzlaff, J. D. Dunitz, C. M. Gramaccioni, H. H. Schulz, U. Shmueli, S. C. Abrahams, Atomic displacement parameter nomenclature. Report of a subcommittee on atomic displacement parameter nomenclature. *Acta Crystallogr.* **A52**, 770–781 (1996).
43. C. L. Barros, P. J. P. de Oliveira, F. E. Jorge, A. Canal Neto, M. Campos, Gaussian basis set of double zeta quality for atoms Rb through Xe: Application in non-relativistic and relativistic calculations of atomic and molecular properties. *Mol. Phys.* **108**, 1965–1972 (2010).
44. R. C. de Berrêdo, F. E. Jorge, All-electron double zeta basis sets for platinum: Estimating scalar relativistic effects on platinum(II) anticancer drugs. *J. Mol. Struct. (Theochem)* **961**, 107–112 (2010).
45. S. S. Shapiro, M. B. Wilk, An analysis of variance test for normality (complete samples). *Biometrika* **52**, 591–611 (1965).
46. P. Munshi, T. S. Thakur, T. N. Guru Row, G. R. Desiraju, Five varieties of hydrogen bond in 1-formyl-3-thiosemicarbazide: An electron density study. *Acta Crystallogr.* **B62**, 118–127 (2006).
47. B. Zarychta, J. Zaleski, J. Kyzioł, Z. Daszkiewicz, C. Jelsch, Charge-density analysis of 1-nitroindoline: Refinement quality using free *R* factors and restraints. *Acta Crystallogr.* **B67**, 250–262 (2011).
48. Y.-S. Chen, A. I. Stash, A. A. Pinkerton, Chemical bonding and intermolecular interactions in energetic materials: 1,3,4-Trinitro-7,8-diazapentalene. *Acta Crystallogr.* **B63**, 309–318 (2007).
49. A. Nassour, M. Kubicki, J. Wright, T. Borowiak, G. Dutkiewicz, C. Lecomte, C. Jelsch, Charge-density analysis using multipolar atom and spherical charge models: 2-Methyl-1,3-cyclopentanedione, a compound displaying a resonance-assisted hydrogen bond. *Acta Crystallogr.* **B70**, 197–211 (2014).
50. M. Slouf, A. Holy, V. Petříček, I. Cisarova, Charge density study of hydrogen [(2,4-diaminopyrimidin-1-yl)methyl]phosphonate monohydrate. *Acta Crystallogr.* **B58**, 519–529 (2002).
51. P. Munshi, T. N. Guru Row, Electron density study of 2H-chromene-2-thione. *Acta Crystallogr.* **B58**, 1011–1017 (2002).
52. R. Bianchi, G. Gervasio, G. Viscardi, Experimental electron-density study of 4-cyanoimidazolium-5-olate at 120 K. *Acta Crystallogr.* **B54**, 66–72 (1998).
53. R. Janicki, P. Starynowicz, Charge density distribution in aminomethylphosphonic acid. *Acta Crystallogr.* **B66**, 559–567 (2010).
54. H.-B. Bürgi, S. C. Capelli, A. E. Goeta, J. A. K. Howard, M. A. Spackman, D. S. Yufit, Electron distribution and molecular motion in crystalline benzene: An accurate experimental study combining CCD X-ray data on  $\text{C}_6\text{H}_6$  with multitemperature neutron-diffraction results on  $\text{C}_6\text{D}_6$ . *Chem. Eur. J.* **8**, 3512–3521 (2002).
55. E. A. Zhurova, A. A. Pinkerton, Chemical bonding in energetic materials:  $\beta$ -NTO. *Acta Crystallogr.* **B57**, 359–365 (2001).
56. M. Malecka, L. Chęcińska, A. Rybarczyk-Pirek, W. Morgenroth, C. Paulmann, Electron density studies on hydrogen bonding in two chromone derivatives. *Acta Crystallogr.* **B66**, 687–695 (2010).
57. B. Dittrich, C. B. Hübschle, J. J. Holstein, F. P. A. Fabbiani, Towards extracting the charge density from normal-resolution data. *J. Appl. Crystallogr.* **42**, 1110–1121 (2009).
58. A. Meents, B. Dittrich, S. K. J. Johnas, V. Thome, E. F. Weckert, Charge-density studies of energetic materials: CL-20 and FOX-7. *Acta Crystallogr.* **B64**, 42–49 (2008).
59. Y. Bibila Mayaya Bisseyou, N. Bouhaida, B. Guillot, C. Lecomte, N. Lugan, N. Ghermani, C. Jelsch, Experimental and database-transferred electron-density analysis and evaluation of electrostatic forces in coumarin-102 dye. *Acta Crystallogr.* **B68**, 646–660 (2012).
60. B. Dittrich, T. Koritsánszky, M. Grosche, W. Scherer, R. Flaig, A. Wagner, H. G. Krane, H. Kessler, C. Riemer, A. M. M. Schreurs, P. Luger, Reproducibility and transferability of topological properties; experimental charge density of the hexapeptide cyclo-(D,L-Pro)<sub>2</sub>-(L-Ala)<sub>4</sub> monohydrate. *Acta Crystallogr.* **B58**, 721–727 (2002).
61. R. Guillot, N. Muzet, S. Dahanoui, C. Lecomte, C. Jelsch, Experimental and theoretical charge density of DL-alanyl-methionine. *Acta Crystallogr.* **B57**, 567–578 (2001).
62. R. Flaig, T. Koritsánszky, D. Zobel, P. Luger, Topological analysis of the experimental electron densities of amino acids. 1. D,L-aspartic acid at 20 K. *J. Am. Chem. Soc.* **120**, 2227–2238 (1998).
63. R. Flaig, T. Koritsánszky, B. Dittrich, A. Wagner, P. Luger, Intra- and intermolecular topological properties of amino acids: A comparative study of experimental and theoretical results. *J. Am. Chem. Soc.* **124**, 3407–3417 (2002).
64. V. G. Tsirelson, A. I. Stash, V. A. Potemkin, A. A. Rykounov, A. D. Shutalev, E. A. Zhurova, V. V. Zhurov, A. A. Pinkerton, G. V. Gurskaya, V. E. Zavadnik, Molecular and crystal properties of ethyl 4,6-dimethyl-2-thioxo-1,2,3,4-tetrahydropyrimidine-5-carboxylate from experimental and theoretical electron densities. *Acta Crystallogr.* **B62**, 676–688 (2006).
65. L. J. Farrugia, P. Kočovský, H. M. Senn, S. Vyskočil, Weak intra- and intermolecular interactions in a binaphthol imine: An experimental charge-density study on ( $\pm$ )-8'-benzhydrylideneamino-1,1'-binaphthyl-2-ol. *Acta Crystallogr.* **B65**, 757–769 (2009).
66. V. Pichon-Pesme, H. Lachekar, M. Souhassou, C. Lecomte, Electron density and electrostatic properties of two peptide molecules: Tyrosyl-glycyl-glycine monohydrate and glycyl-aspartic acid dihydrate. *Acta Crystallogr.* **B56**, 728–737 (2000).
67. F. Benabicha, V. Pichon-Pesme, C. Jelsch, C. Lecomte, A. Khmou, Experimental charge density and electrostatic potential of glycyl-L-threonine dihydrate. *Acta Crystallogr.* **B56**, 155–165 (2000).
68. P. Śledź, R. Kamiński, M. Chruszcz, M. D. Zimmerman, W. Minor, K. Woźniak, An experimental charge density of HEPES. *Acta Crystallogr.* **B66**, 482–492 (2010).
69. L. Chęcińska, S. Grabowsky, M. Malecka, A. J. Rybarczyk-Pirek, A. Józwiak, C. Paulmann, P. Luger, Experimental and theoretical electron-density study of three isoindole derivatives: Topological and Hirshfeld surface analysis of weak intermolecular interactions. *Acta Crystallogr.* **B67**, 569–581 (2011).
70. D. Förster, A. Wagner, C. B. Hübschle, C. Paulmann, C. P. Luger, Charge density of L-alanyl-glycyl-L-alanine based on X-ray data collection periods from 4 to 130 hours. *Z. Naturforsch.* **62**, 696–704 (2007).
71. S. Grabowsky, R. Kalinowski, M. Weber, D. Förster, C. Paulmann, P. Luger, Transferability and reproducibility in electron-density studies—Bond-topological and atomic properties of tripeptides of the type L-alanyl-L-alanine. *Acta Crystallogr.* **B65**, 488–501 (2009).
72. R. Kalinowski, B. Dittrich, C. B. Hübschle, C. Paulmann, P. Luger, Experimental charge density of L-alanyl-L-prolyl-L-alanine hydrate: Classical multipole and invariom approach, analysis of intra- and intermolecular topological properties. *Acta Crystallogr.* **B63**, 753–767 (2007).
73. L. Chęcińska, S. Mebs, C. B. Hübschle, D. Förster, W. Morgenroth, P. Luger, Reproducibility and transferability of topological data: Experimental charge density study of two modifications of L-alanyl-L-tyrosyl-L-alanine. *Org. Biomol. Chem.* **4**, 3242–3251 (2006).
74. B. Dittrich, E. Sze, J. J. Holstein, C. B. Hübschle, D. Jayatilaka, Crystal-field effects in L-homoserine: Multipoles versus quantum chemistry. *Acta Crystallogr.* **A68**, 435–442 (2012).
75. B. Dittrich, J. J. McKinnon, J. E. Warren, Improvement of anisotropic displacement parameters from invariom-model refinements for three L-hydroxylysine structures. *Acta Crystallogr.* **B64**, 750–759 (2008).
76. B. Dittrich, P. Munshi, M. A. Spackman, Redetermination, invariom-model and multipole refinement of L-ornithine hydrochloride. *Acta Crystallogr.* **B63**, 505–509 (2007).

77. R. Flaig, T. Koritsánszky, J. Janczak, H.-G. Krane, W. Morgenroth, P. Luger, Fast experiments for charge-density determination: Topological analysis and electrostatic potential of the amino acids L-Asn, DL-Glu, DL-Ser, and L-Thr. *Angew. Chem. Int. Ed.* **38**, 1397–1400 (1999).
78. S. Scheins, B. Dittrich, M. Messerschmidt, C. Paulmann, P. Luger, Atomic volumes and charges in a system with a strong hydrogen bond: L-Tryptophan formic acid. *Acta Crystallogr.* **B60**, 184–190 (2004).
79. S. Scheins, M. Messerschmidt, P. Luger, Submolecular partitioning of morphine hydrate based on its experimental charge density at 25 K. *Acta Crystallogr.* **B61**, 443–448 (2005).
80. P. Munshi, T. N. Guru Row, Intra- and intermolecular interactions in small bioactive molecules: Cooperative features from experimental and theoretical charge-density analysis. *Acta Crystallogr.* **B62**, 612–626 (2006).
81. J. Lübben, C. Volkman, S. Grabowsky, A. Edwards, W. Morgenroth, F. P. A. Fabbiani, G. M. Sheldrick, B. Dittrich, On the temperature dependence of  $H-U_{iso}$  in the riding hydrogen model. *Acta Crystallogr.* **A70**, 309–316 (2014).
82. S. Dohaoui, C. Jelsch, J. A. K. Howard, C. Lecomte, Charge density study of *N*-acetyl-L-tyrosine ethyl ester monohydrate derived from CCD area detector data. *Acta Crystallogr.* **B55**, 226–230 (1999).
83. R. Kamiński, S. Domagała, K. N. Jarzemska, A. A. Hoser, W. F. Sanjuan-Szklarz, M. J. Gutmann, A. Makal, M. Malińska, J. M. Bąk, K. Woźniak, Statistical analysis of multipole-model-derived structural parameters and charge-density properties from high-resolution X-ray diffraction experiments. *Acta Crystallogr.* **A70**, 72–91 (2014).
84. A. Paul, M. Kubicki, C. Jelsch, P. Durand, C. Lecomte, *R*-free factor and experimental charge-density analysis of 1-(2'-aminophenyl)-2-methyl-4-nitroimidazole: A crystal structure with  $Z' = 2$ . *Acta Crystallogr.* **B67**, 365–378 (2011).
85. A. Poulain, E. Wenger, P. Durand, K. N. Jarzemska, R. Kamiński, P. Fertey, M. Kubicki, C. Lecomte, Anharmonicity and isomorphous phase transition: A multi-temperature X-ray single-crystal and powder diffraction study of 1-(2'-aminophenyl)-2-methyl-4-nitroimidazole. *IUCr* **1**, 110–118 (2014).
86. E. A. Zhurova, V. G. Tsirelson, V. V. Zhurov, A. I. Stash, A. A. Pinkerton, Chemical bonding in pentaerythritol at very low temperature or at high pressure: An experimental and theoretical study. *Acta Crystallogr.* **B62**, 513–520 (2006).
87. V. V. Zhurov, E. A. Zhurova, A. I. Stash, A. A. Pinkerton, Importance of the consideration of anharmonic motion in charge-density studies: A comparison of variable-temperature studies on two explosives, RDX and HMX. *Acta Crystallogr.* **A67**, 160–173 (2011).
88. J. J. Holstein, P. Luger, R. Kalinowski, S. Mebs, C. Paulmann, B. Dittrich, Validation of experimental charge densities: Refinement of the macrolide antibiotic roxithromycin. *Acta Crystallogr.* **B66**, 568–577 (2010).
89. B. Dittrich, M. A. Spackman, Can the interaction density be measured? The example of the non-standard amino acid sarcosine. *Acta Crystallogr.* **A63**, 426–436 (2007).
90. D. M. M. Jaradat, S. Mebs, L. Chęćńska, P. Luger, Experimental charge density of sucrose at 20 K: Bond topological, atomic, and intermolecular quantitative properties. *Carbohydr. Res.* **342**, 1480–1489 (2007).
91. C. B. Hübschle, B. Dittrich, S. Grabowsky, M. Messerschmidt, P. Luger, Comparative experimental electron density and electron localization function study of thymidine based on 20 K X-ray diffraction data. *Acta Crystallogr.* **B64**, 363–374 (2008).
92. H. Birkedal, D. Madsen, R. H. Mathiesen, K. Knudsen, H.-P. Weber, D. Pattison, D. Schwarzenbach, The charge density of urea from synchrotron diffraction data. *Acta Crystallogr.* **A60**, 371–381 (2004).

**Acknowledgments:** We thank J. Beckmann (University of Bremen) and J. A. K. Howard (Durham University) for their suggestions, as well as C. B. Hübschle (University of Bayreuth) and V. Arion (University of Vienna) for the donation of experimental structure factors. P. Luger (Free University of Berlin), M. F. Hesse (University of Bremen), W. Morgenroth (DESY, Hamburg), and R. Kalinowski (Free University of Berlin) are acknowledged for their help with the pentaphenyldisiloxane measurements, which took place at synchrotron beamline D3 of the HASYLAB at DESY (Hamburg, Germany). We thank H. Puschmann for initiating collaboration with OlexSys and O. Dolomanov for incorporating HART into Olex2. **Funding:** This work was financially supported by grants from the Australian Research Council (DP110105347 and DE140101330), the Deutsche Forschungsgemeinschaft (Emmy Noether grant GR4451/1-1), and the Polish National Science Centre (MAESTRO decision no. DEC-2012/04/A/ST5/00609). The Interdisciplinary Centre for Mathematical and Computational Modeling at the University of Warsaw (grant no. G53-17) and the Wrocław Centre for Networking and Supercomputing (grant no. 115) are acknowledged for providing computer facilities. **Author contributions:** S.G. is the corresponding author of this work. S.G. and D.J. designed the project, and S.G. coordinated it. M.W. performed all refinements and statistical analyses. P.M.D. and K.W. interpreted and analyzed the statistical results. M.W., S.G., and D.J. wrote the manuscript. **Competing interests:** The authors declare that they have no competing interests. **Data and materials availability:** All data needed to evaluate the conclusions in the paper are present in the paper and/or the Supplementary Materials. Additional data related to this paper may be requested from the authors. Crystallographic meta-data and atomic coordinates have been deposited with the CSD as CIFs (under nos. 1423823 to 1423876 and nos. 1423882 to 1423913) and with the Karlsruhe Inorganic Crystal Structure Database (under no. 430202). CIFs for all refinements have also been uploaded with *Science Advances*. "Raw refinement and statistical data" as a separate PDF document has been deposited at [www.figshare.com](http://www.figshare.com) under <https://dx.doi.org/10.6084/m9.figshare.3205588.v1>.

Submitted 1 February 2016

Accepted 28 April 2016

Published 27 May 2016

10.1126/sciadv.1600192

**Citation:** M. Woźnińska, S. Grabowsky, P. M. Dominiak, K. Woźniak, D. Jayatilaka, Hydrogen atoms can be located accurately and precisely by x-ray crystallography. *Sci. Adv.* **2**, e1600192 (2016).



This article is published under a Creative Commons license. The specific license under which this article is published is noted on the first page.

For articles published under [CC BY](#) licenses, you may freely distribute, adapt, or reuse the article, including for commercial purposes, provided you give proper attribution.

For articles published under [CC BY-NC](#) licenses, you may distribute, adapt, or reuse the article for non-commercial purposes. Commercial use requires prior permission from the American Association for the Advancement of Science (AAAS). You may request permission by clicking [here](#).

***The following resources related to this article are available online at <http://advances.sciencemag.org>. (This information is current as of June 7, 2016):***

**Updated information and services**, including high-resolution figures, can be found in the online version of this article at:

<http://advances.sciencemag.org/content/2/5/e1600192.full>

**Supporting Online Material** can be found at:

<http://advances.sciencemag.org/content/suppl/2016/05/24/2.5.e1600192.DC1>

This article **cites 87 articles**, 2 of which you can be accessed free:

<http://advances.sciencemag.org/content/2/5/e1600192#BIBL>

*Science Advances* (ISSN 2375-2548) publishes new articles weekly. The journal is published by the American Association for the Advancement of Science (AAAS), 1200 New York Avenue NW, Washington, DC 20005. Copyright is held by the Authors unless stated otherwise. AAAS is the exclusive licensee. The title *Science Advances* is a registered trademark of AAAS